16

Polymer Crystallization Under High Cooling Rate and Pressure: A Step Towards Polymer Processing Conditions

Andrea Sorrentino, Felice De Santis, and Giuseppe Titomanlio

Department of Chemical and Food Engineering, University of Salerno, Via Ponte don Melillo, I-84084 Fisciano (SA) – Italy
asorrentino@unisa.it, fedesantis@unisa.it, gtitomanlio@unisa.it

Abstract. Even if many efforts have been spent on the explanation of the mechanisms involved during the polymer crystallization in typical industrial processing conditions, they are still only partially understood. Up to now, due to the remarkable experimental difficulties, in literature only few systematic works have been focused on the effect of high cooling rates and/or solidification pressure on the mechanical and physical properties of the semi-crystalline polymers. In this work, we present two experimental apparatuses, designed and assembled with the aim of obtaining polymer samples under controlled temperature and pressure histories. High cooling rates and pressure, comparable with those experienced by the polymer during industrial processes, were attained in order to produce polymer samples with different morphologies. Exemplar results obtained with Syndiotactic Polystyrene (sPS) show that high cooling rates as well as external pressure are important factors for inducing changes in crystalline polymeric structures.

16.1 Introduction

Crystallization plays an important role in industrial processing of semi-crystalline resins. It strongly affects rheological properties of polymer melts and solutions and influences mechanical and barrier properties of solid objects. Therefore, realistic modeling of technological processes (injection molding, film casting, melt spinning, etc.) involving crystallizable polymers requires that crystallization during processing has to be taken into account.

Unfortunately, during processing operations, crystallization takes place under conditions of cooling rates and pressure much severe than those accessible to available analytical apparatuses (Table 16.1).

An enlargement of the experimental data range is obviously of interest also for a better understanding of basic phenomenon. Indeed, despite the large number of papers concerning polymer crystallization, the role of mesomorphic phase in the formation of the crystalline structures is not completely

A. Sorrentino et al.: *Polymer Crystallization Under High Cooling Rate and Pressure: A Step Towards Polymer Processing Conditions*, Lect. Notes Phys. **714**, 329–344 (2007)
DOI 10.1007/3-540-47307-6_16

Table 16.1. Processing Conditions versus Available experimental range

Analysis	Apparatus	Range Available	Processing Conditions
Calorimetric	DSC – DTA	Cooling rates $<8\,\mathrm{K/s}$ Pressure $<100\,\mathrm{bar}$	Cooling rates $\in 1 \div 1000\,\mathrm{K/s}$
Volumetric	PVT	Cooling rates $<0.03\,\mathrm{K/s}$	Pressure $\in 1 \div 1000\,\mathrm{bar}$
Rheological	Rheometers (rotational, capillary, etc.)	Cooling rates $<0.5\,\mathrm{K/s}$ Shear rates $<1000\,\mathrm{s}^{-1}$	Shear rates $\in 500 \div 10^5\,\mathrm{s}^{-1}$

clear [1, 2]. It is recognized from many experimental evidences, however, that the metastability of morphological entities plays a major role, leading to reorganization, annealing, re-crystallization, super-heating, etc. [3]. One way of avoiding reorganization effects is to increase the scan rate, whereas the amount of reorganization can be established by varying the scan rate.

During crystallization, it is very useful to study the interaction between processing conditions and crystallization-morphology [4]. A great deal of progress can be made by combining different techniques and conducting the various measurements under the same conditions, particularly on samples which experienced the same thermal history. The improvement of simultaneous measurement techniques, such as X-ray, small angle light scattering (SALS), infrared spectroscopy (IR), and dielectric spectroscopy, would be of extraordinary help for providing additional information for the interpretation of solidification/melting transitions, especially for measurements coming from fast crystallization process.

Fast and non-contact methods for the analysis of morphologies evolution during a fast process are highly attractive and, from this point of view, light transmission appears the more promising. In contrast to other methods (calorimetry, X-ray diffraction, densitometry), in fact, measurements of light intensity are very fast, economical, and can be applied in situations (rapid cooling, flow) when other methods are not adequate.

First attempts of monitoring polymer crystallization by light depolarization technique were made in 50s and early 60s [5–7]. Ding and Spruiell [8–10] modified the use of the depolarized light microscopy (DLM) technique so that it could be used to study the overall non-isothermal crystallization kinetics of semi-crystalline polymers under cooling conditions similar to those occurring in the melt-spinning process. On the basis of transmitted light intensity data, they corrected for the scattering that may be present in the transmitted depolarized light intensity data obtained as a result of crystallization in a sample held in a temperature-controlled hot stage. However, the application of the analysis suggested by Ding and Spruiell to some results obtained by Brucato et al. [11] gave rise to unacceptable results as the relative light intensity index shows a maximum during monotonous cooling, which is not an acceptable

evolution for a variable that is supposed to represent crystallinity. Lamberti et al. [12] proposed a simple macroscopic model describing the main interactions between a light beam and a semi-crystalline polymer. The proposed model was found to be able to reproduce the observed experimental behavior of light intensities and it was validated by comparison with conventional DSC analysis.

Another important variable affecting the crystallization of a polymer material is the pressure under which it takes place. Basic investigations in this field have been made by Wunderlich and Bassett [13–15]. Their results show that high pressures produce several effects on the properties of polyethylene.

Polyethylene solidified under high pressure usually presents a higher density, a higher melting temperature at atmospheric pressure, a higher crystallinity, and also a peculiar morphology: the formation of a hexagonal phase, intermediate between the stable (orthorhombic) phase and the melt, was evidenced in polyethylene samples crystallized under pressure higher than 3000 bar [14]. Up to now, there are only a limited number of other polymers whose morphology has been studied at elevated pressures [16–18].

However, these investigations were carried out under quasi-isothermal conditions and furthermore pressures are extremely high (typically 2000 bar) with respect to the pressures normally adopted in industrial processes. This implies that the results obtained may not be directly applicable to polymer processing operations, which often involve very high thermal gradients and cooling rates.

Major problems encountered when one tries to apply simultaneous high cooling rates and high pressure rely on the relatively large mass of the sample to ensure the reliability of the data obtained, the hydrostatic character of the stress field applied and the safety of the experimental apparatus.

The effect of pressure on melting temperature represents the largest consequence on kinetics; however, it is not the sole effect on crystallization. Few papers reported some interesting but contradictory observations regarding the actual pressure effect on crystallization at constant super-cooling. Wunderlich [19] reported that crystallization of polyethylene was delayed at elevated pressure (at about 5000 bar). In contrast, it has been reported [20] for a high-density polyethylene that the rate of crystallization was increased with increasing pressure at constant super-cooling. Zoller [21] noted the same tendency as reported by Wunderlich for polyethylene terephthalate, and yet, this effect was not observed for polypropylene and polyamide 6,6.

Thus, also in this case an increase in the quantity and quality of the available experimental data can help to remove ambiguity and aid to understand the polymer solidification in more detail. Interesting examples of the complex morphology that can be achieved in a transformation process come from the structural analysis of injection molded samples in Syndiotactic Polystyrene [22–25].

Exemplar micrographs of injection molded sPS samples (about 2 mm thick) are reported in Fig. 16.1 [25, 26]. These samples show a distribution along thickness direction of transparent, amorphous layers (white layers in

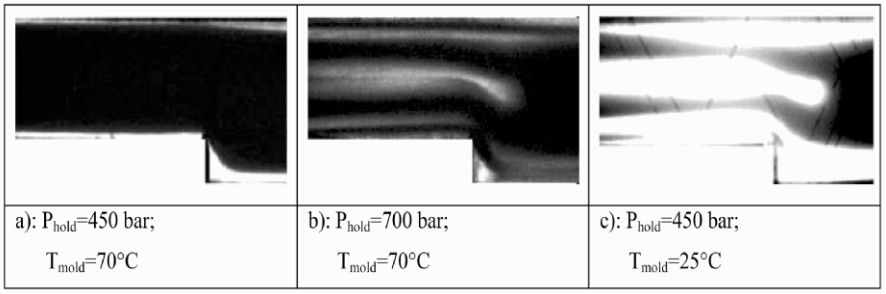

Fig. 16.1. Micrographs of injection molded samples in polarized light. The distinctive processing conditions are reported in label (P_{hold} = Packing pressure; T_{mold} = Mold surface temperature)

the micrograph reported in Fig. 16.1) and opaque, crystalline layers (black layer in the micrograph). Thus, under appropriate processing conditions, the amorphous skin-semicrystalline intermediate layer-amorphous core multilayer structures can be found across the thickness direction. This complex multilayered structure is strongly dependent on the processing variables. In particular, an increase in the packing pressure produces a considerable enlargement of the amorphous core layer (Fig. 16.1 a → b). Equivalently, a reduction of the molding temperature produces a thickening of all amorphous layers with particular effect on the skin layer (Fig. 16.1 a → c). The situation is further influenced by the stress-induced crystallization. The material exposed to the proper levels of stresses, especially at low temperatures, for a sufficient length of time, is induced to crystallize due to the accelerating influence of stress [23].

The final orientation distribution in the mould piece is dependent on the cooling rate, the injection speed and the packing pressure. All these parameters strongly affect the spectrum of relaxation times and the kinetics of crystallization. On one side, a reliable modeling of the overall crystallization kinetic in all processing conditions is the precondition for a correct description of every industrial processing. On the other side, the success of any computer modeling, however, largely depends on the quality of the input information used for describe the material behavior. The super-position of simultaneous cooling rates, packing pressure and molecular orientation is hard to describe without a capable computer simulation. Certainly, additional efforts are needed to overcome experimental difficulties by improving techniques, by combining complementary techniques, or by choosing the optimal material sample. In this work are shown two experimental techniques able to characterize polymer samples in a wide range of cooling rates and pressures. Experimental characterization of Syndiotactic Polystyrene (sPS) help us to illustrate the importance that high cooling rates and pressure have on the solidification process and hence on the final crystalline texture of common polymeric materials.

16.2 Material and Methods

The studied Syndiotactic Polystyrene (Questra QA101) was supplied by the Dow Chemical Company. The molecular weight characteristics of this material were: $M_w = 320000$ g/mol and $M_w/M_n = 3.9$. sPS is a semi-crystalline polymer, which stimulates interest because of its impressive material properties, its unusual polymorphism and its sensibility to processing conditions. Up to now, four different phases were obtained and characterized [27]. In particular, the α and β forms contain chains in planar zigzag conformation and can be obtained either by melt crystallization or by annealing of amorphous samples at proper temperatures [28]. The crystallization of the α form is favored by fast cooling from the melt, by low isothermal temperatures or by cold crystallization from the quenched glass. Crystallization at high temperatures (close to the melting temperature) or under a moderate cooling rate from the melt leads to formation of the β form; otherwise, always a mixture of the two phases (α and β) is obtained. In addition, the sPS presents peculiar relative values of the densities of the different phases. In fact, the crystalline density of the α phase, $1.033\,\mathrm{g/cm^3}$, calculated from the parameters of the unit cell, is smaller than the density of the amorphous phase, $1.048\,\mathrm{g/cm^3}$, whereas the predicted density of the β phase, $1.068\,\mathrm{g/cm^3}$, is larger than the density of the amorphous phase [28, 29].

16.2.1 DTA Experiments

Non-isothermal crystallization kinetic of sPS was investigated using a "Mettler 822 DSC" analyzer equipped with a liquid nitrogen cooling accessory. The heat flow and temperature of DTA were calibrated with standard materials, indium and zinc, prior and after the investigation. Nitrogen gas was purged into DTA furnace during the scans to prevent oxidative degradation at high temperature. Sample weights were chosen between 5 and 10 mg. The as-received material was put in the DTA aluminum pans and heated at 310°C for 15 min to erase any thermal history. Non-isothermal crystallization was carried out at various cooling rates ranging between 0.3 and 100 K/min.

16.2.2 High Cooling Rates Device

An innovative apparatus, which is shown in Fig. 16.2, was adopted for achieving fast cooling crystallization tests [11, 30]. It includes a hot (oven zone) section and a quenching zone section. Sample heating is attained by two radiant electric heaters and the cooling system consists of a couple of gas or gas-liquid (typically air and water) operated nozzles, which spray symmetrically both faces of the sample holder. This cooling system was designed as to determine a large range of cooling rates. As shown in Fig. 16.2 the polymer sample, a thin film (50–100 μm), with an embedded thermocouple is confined between two thin cover glasses that act as sample holders. The sandwich, sample –

Fig. 16.2. Quenching device and sample assembly scheme

cover glasses, is fastened to a sliding rod, which can be quickly shifted from the hot to the quenching section.

To the purpose of monitoring the crystallinity evolution, an optical set-up was built and it is schematically shown in Fig. 16.3. A laser beam, past the polarizer, crosses the sandwiched polymer film (the sample in Fig. 16.3) while it is subjected to the cooling treatment. The apparatus is able to carry out simultaneous detections of both the depolarized beam intensity and the overall beam intensity, downstream from the film under analysis. The results of these measurements can be related to sample crystallinity content, on the basis of optical properties of each phase [31]. The apparatus can reach very high cooling rates (up to few thousands K/s @ 200°C) by spraying a mixture of air and water on the sample surfaces. Under these conditions, however, the water droplets interact with the laser, strongly reducing the signal intensity detected; it obviously leads to some difficulties in the analysis of results.

16.2.3 Rapid Solidification Under Pressure

Another homemade apparatus was designed and assembled with the aim of obtaining polymer samples solidified under known temperatures and pressure histories [32, 33]. The apparatus, based on the confining fluid techniques, applies hydrostatic pressure on the sample during fast solidification.

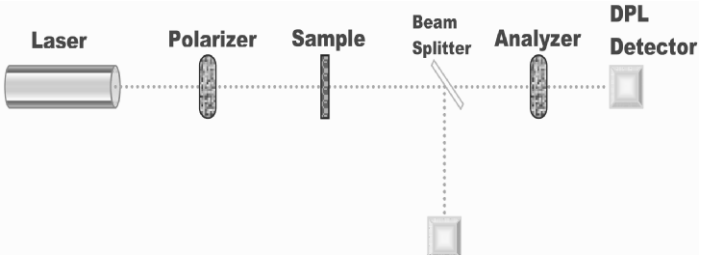

Fig. 16.3. Optical assembly detection scheme

Characterization of samples solidified under known temperature and pressure histories allows correlating temperature and pressure histories to final morphology and properties. The main objective is to attain cooling rates and pressures higher than those achieved by the other available experimental devices which applying hydrostatic pressure on the solid samples. This objective was already achieved: polymeric samples were solidified under simultaneous 1250 bar and 40 K/s (measured at 200°C), see below (Fig. 16.4). The polymeric samples, thin films (100-300 μm), were firstly melted and maintained at the desired temperature and pressure for a suitable time. The samples were then cooled down to ambient temperature under various cooling rates, while the pressure was maintained constant; the values of both temperature and pressure were monitored constantly during the tests.

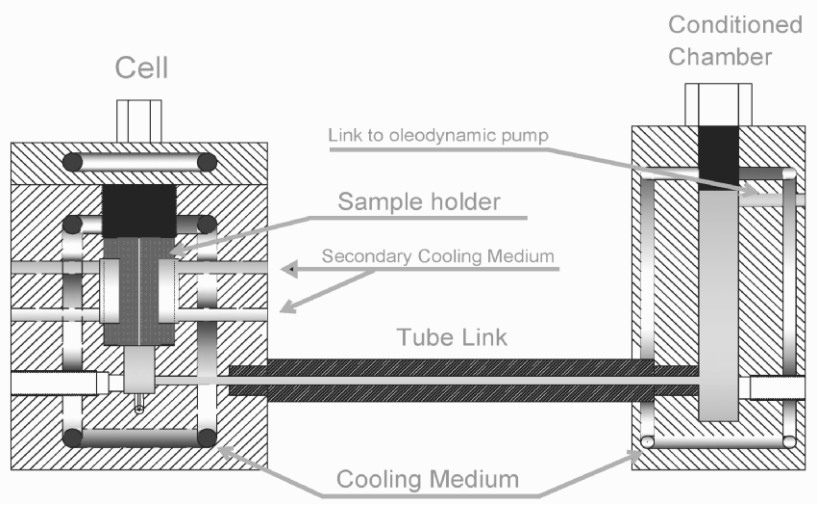

Fig. 16.4. Schematic representation of the apparatus for solidification under pressure

The equipment, schematized in Fig. 16.4, consists of a heated-pressurized steel cylinder, named "cell", where the polymer is confined in mineral oil, and a separate conditioned chamber where the pressure is applied on the pressure-transmitting medium by means of a manual oleodynamic pump. A long thermal conditioned steel tube links the secondary chamber and the pressurized cell. Such a construction avoids any overheating of the pump elements. The insert, that contains the polymer sample, is also cylindrical and can easily be removed from the cell. It is made of a copper-beryllium (98/2) alloy, that has good mechanical properties and elevated thermal conductivity that guarantees a uniform sample cooling. Inserts of different geometry were available: the more excavated allowing the higher cooling rates (Fig. 16.5).

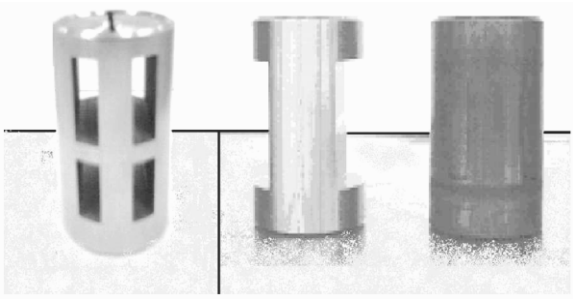

Fig. 16.5. Pictures of inserts with various geometries. Maximum cooling rate accessible @ 200°C: a) 40 K/s; b) 5 K/s; c) 1.5 K/s

16.2.4 Morphological Characterization

All the samples obtained were analyzed by means of X-ray analysis and densitometry.

X-ray diffraction spectra were recorded with a "Philips PW 1830" X-ray generator and a flat camera with a sample-to-film distance of 220 mm (Ni-filtered Cu-Kα radiation) and 1 hour exposure time. A "Fujifilm MS 2025" imaging plate (0.1 mm/pitch) and a "Fuji Bio-imaging Analyzer System", were used to gather and digitalize the diffraction patterns. The degree of crystallinity X_c from the WAXD was evaluated by the spectra according to the Hermans-Weidinger methods [34].

Density was measured by using a gradient column prepared from water and a water solution of sodium chloride. The column was calibrated with glass beads of known density. The samples were placed in the column and allowed to equilibrate for 60 min before the measure were taken. The experimental density of the samples was analyzed with the following model:

$$\rho = \rho_\alpha X_\alpha + \rho_\beta X_\beta + \rho_a(1 - X_\alpha - X_\beta) \tag{16.1}$$

where ρ, ρ_a, ρ_α and ρ_β are the density of the sample, the amorphous phase, the α phase and the β phase, respectively. X_α and X_β are the volume fraction of α and β phase, respectively. Equation (16.1) allows calculation of the volume fraction of α and β phases once total degree of crystallinity $(X_\alpha + X_\beta)$ is evaluate from WAXD measurements, with the proviso that the crystallinity density of single phases are known.

16.3 Experimental Results

Typical results of the quenching experiments, i.e. both overall and depolarized light intensities as well as temperature are reported in Fig. 16.6 as function of

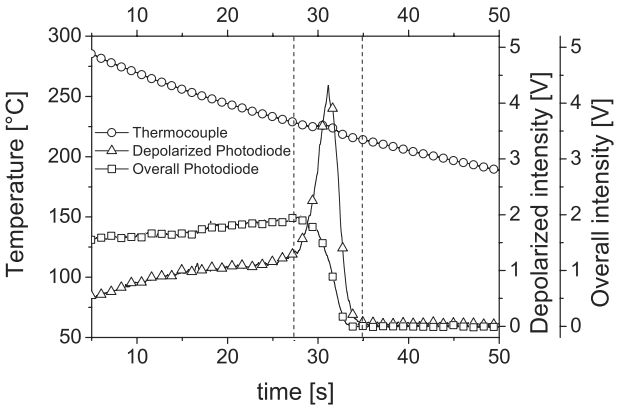

Fig. 16.6. Typical signals output of sPS experiments and values of overall and depolarized intensities adopted for parameters identification

time. The overall light intensity (measured at time t, downstream of a film of thickness S), $I_O(t, S)$ initially shows a quasi constant value. When crystallization starts the light intensity decreases, reaching a new constant level, lower than the initial one. The depolarized light intensity, $I_D(t, S)$, initially shows a constant value, likewise the overall light intensity, then it increases, attains a maximum and then decreases, achieving a new constant level, lower than the initial one. The evolution of the temperature recorded just inside the sample is also reported in Fig. 16.6. A perturbation in the temperature signal is well evident in correspondence of the maximum in the depolarized light intensity. Probably, it is due to the heat generation during the crystallization. From the picture, it is possible to identify the characteristic temperature values of the process (i.e. the starting and the crystallization end).

The temperature at which the crystallization started, were it attained the 50% (for the quenching experiments were the polarized light intensity attained its maximum) and where it finished are reported in the Fig. 16.7, for non-isothermal tests, carried out both in the DTA and in the quenching device. For graphic purpose, the experimental tests carried out at a non-constant cooling rate (quenching experiments) were identified with the cooling rate recorded at 200°C. This temperature was chosen because the large part of the crystallization process takes place close to this temperature. The densities of the solidified samples are reported in Fig. 16.7 where the density levels of α, β and amorphous phases are also shown. As expected, the DTA temperature range where the crystallization takes place increases strongly with the cooling rate and moves to lower temperatures. This behavior is common at both enthalpic and optical results.

The DTA results do not fit with the results coming from optics signal. In particular, the end of the process seems anticipated in the quenching experiments. It can be due to many reasons. First of all, the DTA experiments

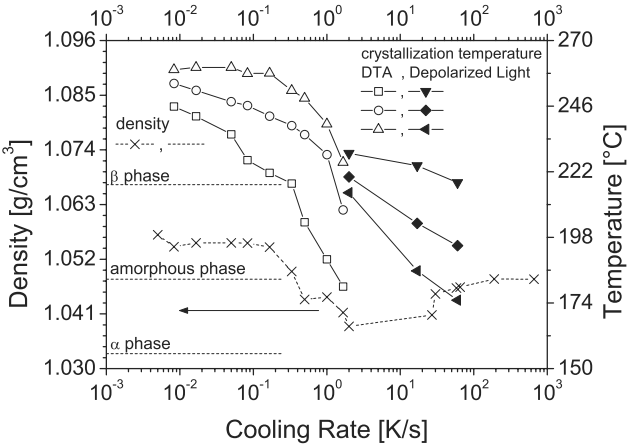

Fig. 16.7. Final Samples Density and Crystallization temperatures as a function of cooling rate @ 200°C. *Open symbols* are data taken from calorimetric (DTA) trace. *Full symbols* are data taken from Depolarized Light measurements

are carried out at constant cooling rates, whereas quenching experiments are obtained with an exponential temperature decrease. In the case of DTA, also the time lag of the instrument must be taken into account. Many corrections were proposed in order to correct enthalpic traces [35,36]. The DTA data proposed in Fig. 16.7 are shown without any type of correction. However, despite the correction proposed, the effect produces generally both a non symmetric shrinkage and a small shift of the crystallization peak versus higher temperature. This effect is quite proportional to the sample mass and cooling rate. The last possibility of misfit between DTA curves and optical signal, is that the last part of the crystallization process, even if it produces a thermal response, does not show appreciable optic effects. It is common in all situations when one tries compare experimental results taken with different techniques. In general, cannot be expected that the same definition of crystallinity holds for all experimental signal. Different techniques present dissimilar sensibility to material properties; it means that for a correct characterization of the polymeric samples the crystallinity degree is not sufficient for a complete characterization.

Densities of final samples are also reported in Fig. 16.7. As the cooling rate increases, the density of the samples clearly decreases from values close to the β phase, to values close to the α phase. This is in good agreement with well known literature results according to an increase of cooling rate produces an increase in α content in the solid sample. The density of the solidified solid samples starts to decrease when the crystallization starts at temperatures lower than 258°C, namely when the cooling rate is higher than 0.2 K/s. It attains a minimum (close to the α phase density) between 2 and 20 K/s and it increases toward the amorphous value for larger densities. Such

a dependence of the densities of solidified samples on cooling rate is consistent with their phase composition (α, β and amorphous) determined by X-rays.

These are plotted versus cooling rate recorded at 200°C in Fig. 16.8. Total crystallinity content goes from the value $X_{\max} = 60\%$ vol/vol to zero in less than two orders of magnitude of the cooling rate. At cooling rate of about 50 K/s the crystallinity of the solid sample obtained undergoes a sharp decrease; it drops to about 10% of $X_{\max}$ at 200 K/s and nearly to zero at cooling rate of 600 K/s.

As also shown in Fig. 16.8, the β phase content decreases continuously with cooling rate, whereas the α phase content shows a monotonic increase up to about 1 K/s (cooling rate transition between DTA and quenching experiments). In particular, the α phase starts to be predominant in the final morphology of the samples when the crystallization process takes place at temperature lower than 250°C or equivalently under cooling rates higher than 0.5 K/s. Indeed, the effect of cooling rates on the final morphology of sPS samples is rather complex and difficult to predict starting from experimental data recorded at low cooling rates. This behavior is still more complex in presence of high pressures.

Final phase composition (α + β) of sPS samples solidified in the apparatus described in this work at 5 K/s @ 200°C are reported in Fig. 16.9. These were evaluated on the basis of X-ray diffraction characterization [33]. The data clearly show a reduction in the overall final crystallinity by effect of an increase of solidification pressure from 0 to 450 bar. At room pressure (Fig. 16.8) overall final crystallinity degree in the solid samples gradually decreases with cooling rate, and α phase is predominant at 5 K/s. The effect of an increasing pressure

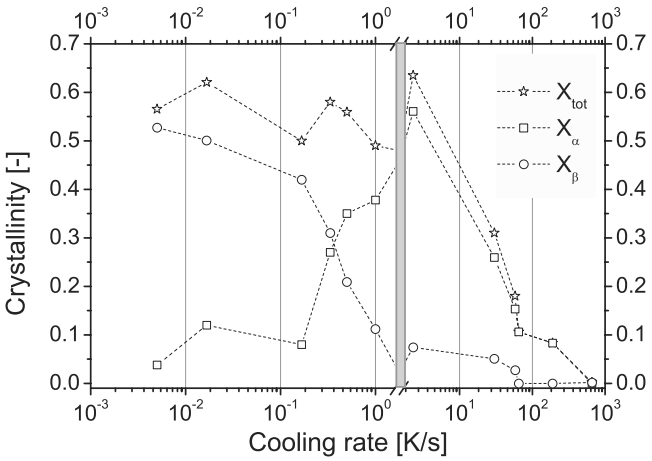

Fig. 16.8. Phase distribution in non-isothermal experiments on sPS samples. The gray band divides DTA experiments from quenching experiments

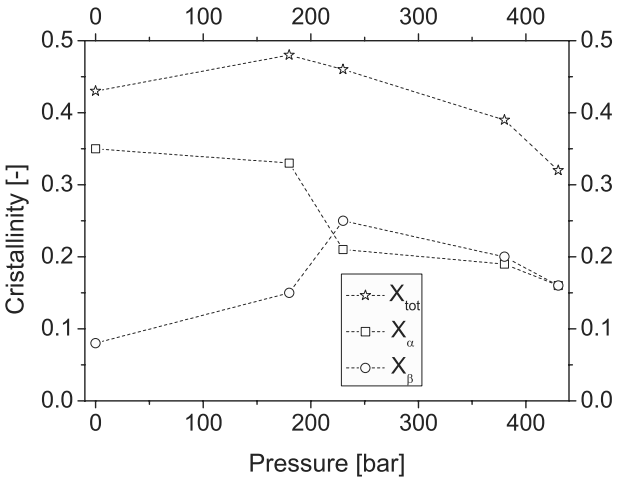

Fig. 16.9. Phase distribution in high pressure non-isothermal crystallization experiments. The solidifications were carried out at a cooling rate of 5 K/s @ 200°C

is toward an increase of the β phase content. Indeed, as expected, an increase in the solidification pressure promotes the content of the higher density phase.

16.4 Discussion

Growth rate data as well as overall crystallization kinetic of polymeric material shows a bell shape as a function of temperature with a maximum located between melting temperature and glass transition temperature. This very general behavior cannot be experimentally observed for many fast crystallizing polymers, like PE, iPP, sPS, etc. For these polymers, in fact, standard calorimetric experiments cannot be performed on the time scale of nucleation and crystallization. In general, for commercial polymers this situation is the rule rather than the exception. For this reason, the majority of analysis of the experimental data in terms of kinetic model is carried at temperatures approaching the melting point, where the crystallization rate is dominated by the thermodynamic driving force. The diffusion term parameters (transport process at the interface between the melt and the crystal surface) are generally used as simple fitting parameters. This not only leads to a poor description of the crystallization at temperature close to the glass transition, but also avoids any theoretical conclusion on the diffusion process. The possibility of achieving high cooling rates during the crystallization from the melt can be important also for elucidating complex polymorphic behavior as in the case of sPS.

An interesting connection between stability and kinetics may be also implied from the stability diagram of the sPS, as displayed in Fig. 16.10. The

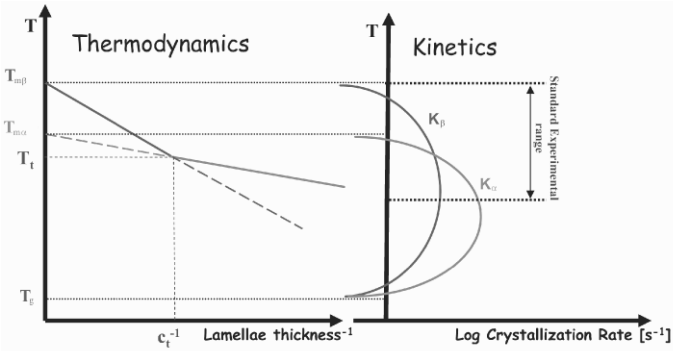

Fig. 16.10. Comparison between Kinetics and stability diagram of the sPS

thermodynamic stability lines of the two phases are reported on the left hand side of the Fig. 16.10 as function of the reciprocal lamellae thickness. At any value of the lamellae thickness, the stable phase is presented as a solid line whereas the meta-stable phase with a broken line. The intersection of the phase lines defines a triple point Q, where all three phases (the melt, α and β crystals) can coexist as stable phases. ¿From the viewpoint of kinetics, the smaller the critical nucleus, the faster the crystallization rate of crystalline phase. The crystallization rate of α form is, thus, expected to be faster than that of β form in the temperature range approaching the glass temperatures and viceversa close to the melting temperature. In the case of sPS, this conclusion has been further approved by the comparison of crystallization kinetics bell shaped curves of the two phases. The maximum crystallization rate of β form was found to be about ten times smaller than that of α form, however at high temperature (close to melting points of the two phases) the relation inverts and crystallization rate of β form become considerably higher than that of the α form [28, 33].

The effect of pressure on the crystallization behavior has been generally attributed to the effect of increasing melting point with pressure, which in turn is equivalent to amplify the degree of super-cooling. However, as reported by Hohne [17,37] this behavior is not true for all the crystal phases. In particular, for the sPS the α phase shows a decrease of the melting point with pressure whereas that of the β phase shows an opposite trends. The opposite behavior of the melting temperature of the two crystal phases with pressure is a consequence of the fact that the density of the amorphous phase is smaller than the density of the β and larger than the density of the α phase. Indeed, the well known Clausius-Clapeyron equation gives for the derivative of the transition temperature with respect to pressure:

$$\frac{\mathrm{d}T_m}{\mathrm{d}p} = T_m \frac{V_c - V_a}{\lambda_f} \tag{16.2}$$

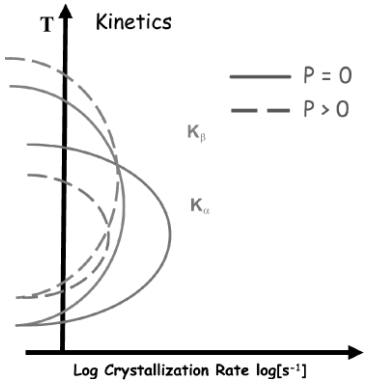

Fig. 16.11. Schematic representation of the crystallization rate as a function of the crystallization temperature and pressure

where T_m is the melting temperature, p the pressure, λ_f the heat of fusion, V_c and V_a the crystalline and amorphous specific volume, respectively.

For the β phase, (16.2) describes a continuous increase of the melting temperature with the pressure and vice versa for the α phase. Also the glass transition temperature was found to increase considerably with pressure. Thus, as sketched in Fig. 16.11, a pressure increase produces a strong reduction in the crystallization range of the α phase, whereas the amplitude of the crystallization range of the β phase is almost unchanged (it is systematically shifted versus higher temperature). The small variation in maximum crystallization value, however, is an indication that crystallization kinetics is even affected by pressure at constant amount of super-cooling [38].

16.5 Conclusions

It is important to grasp properties of polymer systems from the standpoints of the optimal design, the process control, and the savings of energy and resources in polymer industries. In particular, crystallization can dramatically modify dynamics of polymer deformation as well as the properties of the solid material. Even if it seems quite clear for the majority of the researchers in polymer science, for many of them it is surprisingly hard to accept that a correct description of the crystallization in processing conditions requires experimental data covering a wide range of pressures and temperatures, which may change at largely different rates. This work has attempted to analyze the crystallization process of Syndiotactic Polystyrene in a very wide range of experimental conditions. At ambient pressure, the relative degree of α phase increases with the cooling rate up to reaching 100% for cooling rates higher than 1 K/s. For cooling rates higher than 10 K/s, however, the overall final degree of crystallinity in solid samples gradually decreases with increasing

cooling rates. The influence of pressure seems to be mainly limited to the α phase. Indeed, solidification tests under different cooling rates and pressures clearly showed that β phase prevails if sPS samples are solidified under high pressure, whereas β phase is not present at all if samples are solidified at ambient pressure in the whole range of cooling rates of interest for common transformation processing. Albeit, all these behaviors can be explained starting from thermodynamic and kinetics considerations, it is difficult, even impossible to extrapolate from quasi-static laboratory conditions. Crystallization under processing conditions reveals new effects, absent under common laboratory conditions.

References

[1] G. Strobl: Eur. Phys. J. E **18**, 295 (2005)
[2] S.Z.D. Cheng, B. Lotz: Polymer **46**, 8662 (2005)
[3] B. Wunderlich: *Macromolecular physics. Crystal structure, morphology, defect*, vol 1 (Academic Press, New York, 1973)
[4] A. Ziabicki, L. Jarecki, A. Sorrentino: e-Polymers **072** (2004)
[5] K. Fischer, A. Schram Angew Chem **68**, 406 (1956)
[6] J.H. Magill: British Journal of Applied Physics **12**, 618 (1961)
[7] J.H. Magill: Polymer **2**, 221 (1961)
[8] Z. Ding, J.E. Spruiell: J Polym Sci B **34**, 2783 (1996)
[9] Z. Ding, J.E. Spruiell: J Polym Sci B **35**, 1077 (1997)
[10] J.E. Spruiell, P. Supaphol: J Appl Polym Sci **86**, 1009 (2002)
[11] V. Brucato, F. De Santis, A. Giannattasio et al: Macromol. Symp. **185**, 181 (2002)
[12] G. Lamberti, F. De Santis, V. Brucato et al: Appl. Phys. A **78**, 895 (2004)
[13] B. Wunderlich, T. Arakawa: J. Polym. Sci. A **2**, 6397 (1964)
[14] D.C. Bassett, B. Turner: Nature Phys. Sci. **240**, 146 (1972)
[15] D.C. Bassett, S. Block, G.J. Piermarini: J. Appl. Phys. **45**, 4146 (1974)
[16] C. Angelloz, R. Fulchiron, A. Douillard et al: Macromolecules **33**, 4138 (2000)
[17] G.W.H. Hohne, Thermochim. Acta **332**, 115 (1999)
[18] Y. Kojima, M. Takahara, T. Matsuoka et al: J Appl Polym Sci **80**, 1046 (2001)
[19] B. Wunderlich, L. Mellilo: Makromol. Chem. **118**, 250 (1968)
[20] T. Hatakeyama, H. Kanetsuna, H. Kaneda et al: J. Macromol. Sci. **B10**, 359 (1974)
[21] J. He, P. Zoller: J. Polym. Sci. B **32**, 1049 (1994)
[22] A.M. Evans, J.C. Kellar, J. Knowles et al: Polym. Eng. Sci. **37**, 153 (1997)
[23] R.C. Lopez, C.L. Cieslinski, R.D. Wesson: Polymer **36**, 2331 (1995)
[24] Y. Ulcer, M. Cakmak, J. Miao et al: J. Appl. Polym. Sci. **60**, 669 (1996)
[25] R. Pantani, A. Sorrentino, V. Speranza et al: In Proc. PPS 2002, (Taipei Taiwan, 2002)
[26] R. Pantani, A. Sorrentino, V. Speranza et al: In Proc. ICHEAP 6, (Pisa Italy, 2003)
[27] C. De Rosa, G. Guerra, V. Petraccone et al: Polym. J. **23**, 1435 (1991)
[28] A. Sorrentino, M. Tortora V. Vittoria: New developments in syndiotactic polystyrene. In: Recent Res. Devel. Appl. Pol. Sci., (2006): ISBN: 81-308-0129-9

[29] Z. Sun, R.J. Morgan, D.N. Lewis: Polymer **33**, 660 (1992)
[30] F. De Santis: Influence of solidification conditions on structural evolution of thermoplastic polymers. PhD Thesis, University of Palermo, ISBN 88-7676-227-2 (2003)
[31] R.J. Samuels, Structured polymer properties: the identification, interpretation, and application of crystalline polymer structure, (New York: John Wiley 1974)
[32] A. Sorrentino, D. Picarella, R. Pantani et al: Review Scientific Instruments **68**, 245 (2005)
[33] A. Sorrentino: Injection Moulding of Syndiotactic Polystyrene. PhD Thesis, University of Salerno, ISBN 88-7897-001-8 (2005)
[34] L.E. Alexander: X-Ray diffraction Methods in Polymer Science, (Krieger Publishing Co., Florida 1985)
[35] G. Eder, H. Janeschitz-Kriegl In: *Transport Phenomena in Processing*, ed by S.I. Guceri (Technomic Publ. Co. 1993) pp. 1031–1042
[36] V.B.F. Mathot: *Calorimetry and Thermal Analysis* (Hanser, Munich 1994)
[37] C.S.J. van Hooy-Corstjens, G.W.H. Hohne, S. Rastogi: Macromolecules **38**, 1814 (2005)
[38] A. Sorrentino, R. Pantani, G. Titomanlio: In Proc. PPS 21, (Leipzig, Germany 2005)